Sliding Mode Control of Spacecraft with Actuator Dynamics

Yee-Jin Cheon

Abstract: A sliding mode control of spacecraft attitude tracking with actuator, especially reaction wheel, is presented. The sliding mode controller is derived based on quaternion parameterization for the kinematic equations of motion. The reaction wheel dynamic equations represented by wheel input voltage are presented. The input voltage to wheel is calculated from the sliding mode controller and reaction wheel dynamics. The global asymptotic stability is shown using a Lyapunov analysis. In addition the robustness analysis is performed for nonlinear system with parameter variations and disturbances. It is shown that the controller ensures control objectives for the spacecraft with reaction wheels.

Keywords: sliding mode control, quaternion, reaction wheel, switching function, Lyapunov analysis

I. Introduction

The control problems of spacecraft regulation, deployment, and maneuvering, generally pose highly nonlinear characteristics which govern dynamic equations, control rate saturation and its limits[1]. The use of variable structure control for spacecraft maneuvers has been developed for the adequate treatment of such problems and the early contributions to the study of sliding mode control of spacecraft have been done[1,3,4,5]. An optimal control approach for the sliding surface synthesis problem has been developed for a quaternion parameterization[1, 5], and the regulation of spacecraft maneuvers using a Gibbs vector parameterization was developed[3].

In most of research work for spacecraft control, the controllers are designed for external torque. These controllers may be applied to torque device such as thruster. But in real applications, on-time of thruster is very important because system response directly depends on it. In other words, actuator dynamics and characteristics should be considered for real applications. The work for sliding mode control of thruster-controlled spacecraft is found in [8]. Furthermore, the controller whose output is external torque is hardly applied to momentum exchange devices, such as reaction wheels, momentum wheels, and control momentum gyros because momentum exchange device is a motor and it requires voltage as an actuator input.

The spacecraft equipped with momentum exchange devices consists of slow dynamic system for the spacecraft itself and fast dynamic system for the wheel. Also there is momentum exchange between spacecraft system and reaction wheel system without changing overall inertial angular momentum. The angular momentum generated by the reaction wheel is transferred to the spacecraft system and momentum generated by spacecraft rotation affects reaction wheel system. Therefore the controller with actuator dynamics should be considered for real applications. But there are a few research works[1, 6, 8] found for this area. In [1], a sliding mode controller was presented for reaction wheels inputs. However the controller in [1] did not take into account the reaction wheel dynamics.

In this paper, a sliding mode control of spacecraft with actuator dynamics is considered. The sliding mode controller is derived based on quaternion parameterization. A robustness analysis is performed for the nonlinear system with parameter variations and disturbances. The actuator dynamics, especially reaction wheel, is studied and the reaction wheel dynamic equation represented by wheel input voltage is derived. The wheel input voltage for the wheel dynamic equation is obtained from the sliding mode controller. It is shown that the derived controller ensures control objectives irrespective of unmodeled effects and disturbances for spacecraft equipped with reactions wheels.

Manuscript received: April 22, 2001, Accepted: January 15, 2002.
Yee-Jin Cheon: Satellite Electronics Dept., Satellite Division, Korea Aerospace Research Institute P.O.Box 113 Yusung Daejon 305-600, Korea(yjcheon@kari.re.kr)

II. Theoretical background

In this section, the mathematical model of a three-axis stabilized spacecraft is described by dynamic and kinematic equations of motion. The attitude of spacecraft can be described by means of quaternion, defined as follows.

$$\boldsymbol{q} \equiv \begin{bmatrix} \boldsymbol{q}_{13} \\ q_4 \end{bmatrix} \tag{1}$$

with

$$\boldsymbol{q}_{13} \equiv \begin{bmatrix} q_1 \\ q_2 \\ q_3 \end{bmatrix} = \hat{\boldsymbol{n}} \sin(\Phi/2) \tag{2a}$$

$$q_4 = \cos(\Phi/2) \tag{2b}$$

where $\hat{\boldsymbol{n}}$ is an unit vector of corresponding to rotation axis and Φ is the angle of rotation. The quaternion satisfies a normalization constraint.

$$\boldsymbol{q}^T \boldsymbol{q} = \boldsymbol{q}_{13}^T \boldsymbol{q}_{13} + q_4^2 = 1 \tag{3}$$

The quaternion kinematic equations of motion are derived by using spacecraft angular velocity ($\boldsymbol{\omega}$) and expressed by the following [1].

$$\dot{\boldsymbol{q}} = \frac{1}{2}\Omega(\boldsymbol{\omega}) = \frac{1}{2}\Xi(\boldsymbol{q})\boldsymbol{\omega} \tag{4}$$

where $\Omega(\boldsymbol{\omega})$ and $\Xi(\boldsymbol{q})$ are defined as following [1].

$$\Omega(\boldsymbol{\omega}) \equiv \begin{bmatrix} -[\boldsymbol{\omega}\times] & \vdots & \boldsymbol{\omega} \\ \cdots & \vdots & \cdots \\ -\boldsymbol{\omega}^T & \vdots & 0 \end{bmatrix} \tag{5a}$$

$$\Xi(\boldsymbol{q}) \equiv \begin{bmatrix} q_4 \boldsymbol{I}_{3\times3} + [\boldsymbol{q}_{13}\times] \\ \cdots\cdots\cdots\cdots \\ -\boldsymbol{q}_{13}^T \end{bmatrix} \tag{5b}$$

where $\boldsymbol{I}_{n\times n}$ is the $n\times n$ identity matrix. The matrix cross product operator $[\boldsymbol{\omega}\times]$ and $[\boldsymbol{q}_{13}\times]$ are defined by $\boldsymbol{a}\times\boldsymbol{b} = [\boldsymbol{a}\times]\boldsymbol{b}$, and expressed as

$$[\boldsymbol{a}\times] = \begin{bmatrix} 0 & -a_3 & a_2 \\ a_3 & 0 & -a_1 \\ -a_2 & a_1 & 0 \end{bmatrix} \tag{6}$$

The error quaternion between two quaternions, $\boldsymbol{q}$ and the desired quaternion $\boldsymbol{q}_d$, is defined by

$$\delta\boldsymbol{q} \equiv \begin{bmatrix} \delta\boldsymbol{q}_{13} \\ \cdots\cdots \\ \delta q_4 \end{bmatrix} = \boldsymbol{q} \otimes \boldsymbol{q}_d^{-1} \tag{7}$$

where $\otimes$ is the quaternion multiplier, and the inverse quaternion is defined by

$$\boldsymbol{q}_d^{-1} = [-q_1 \quad -q_2 \quad -q_3 \quad q_4]^T \tag{8}$$

Also, the other useful identities are given by [1]

$$\delta\boldsymbol{q}_{13} = \Xi^T(\boldsymbol{q}_d)\boldsymbol{q} \tag{9a}$$

$$\delta q_4 = \boldsymbol{q}^T \boldsymbol{q}_d \tag{9b}$$

The time derivative of Equation (9) is given by

$$\delta\dot{\mathbf{q}}_{13} = \frac{1}{2}\delta q_4 \omega + \frac{1}{2}[\delta\mathbf{q}_{13}\times]\,\omega \tag{10a}$$

$$\delta\dot{q}_4 = -\frac{1}{2}\boldsymbol{\omega}^T \Xi^T(\boldsymbol{q}_d)\boldsymbol{q} = -\frac{1}{2}\boldsymbol{\omega}^T \delta\boldsymbol{q}_{13} \tag{10b}$$

Let $\boldsymbol{J}$ be the rigid body inertia matrix and $\boldsymbol{u}$ be the control torque vector. The Euler's equations of motions for a rigid body are given by

$$\dot{\omega} = f(\omega) + \boldsymbol{J}^{-1}\boldsymbol{u} \tag{11}$$

where,

$$f(\omega) = \mathbf{J}^{-1}[\mathbf{J}\omega\times]\,\omega \tag{12}$$

III. Sliding mode control

The objective of the attitude control is to turn the spacecraft such that the angular velocity of spacecraft, i.e. $\boldsymbol{\omega}$, converges to $\mathbf{0}$, the vector part of the error quaternion, $\delta\boldsymbol{q}_{13}$, converges to $\mathbf{0}$, and the sclar part, δq_4, approaches 1.

Generally, the design strategy of the sliding mode controller consists of two steps[2]:

1. Selection of switching surfaces
2. Sliding condition design

Let us consider a switching surface, a 3-dimensional hyperplane, in the state space of a 6th order system $[\boldsymbol{\omega} \quad \delta\boldsymbol{q}]^T$. The sliding surface is designed in such a way that the spacecraft trajectory, if on the surface, converges to the desired quaternion. However, the motion of spaccraft is not confined to the 3-dimensional hyperplane in general.

Therefore, a control law forcing the spacecraft motion towards the sliding surface is necessary for obtaining stable spacecraft motion. The sliding condition keeps decreasing the distance from the initial state to the sliding surface, such that every solution $\boldsymbol{\omega}$, $\delta\boldsymbol{q}_{13}$ originating outside the sliding surface tends to it. The sliding surface is an invariant set of the spacecraft motion and the attitude trajectory of the system converges to the desired attitude.

1. Selection of switching surfaces

The sliding surface is the subspace of the state space defined below[2]:

$$\boldsymbol{s} \equiv \{(\omega, \delta\boldsymbol{q}_{13}) \mid \boldsymbol{s} = \boldsymbol{0}\} \tag{13}$$

First, let a sliding surface $\boldsymbol{s}$ be defined as

$$\boldsymbol{s} = \boldsymbol{\omega} + \boldsymbol{\Lambda}\,\Xi^T(\boldsymbol{q}_d)\boldsymbol{q} = \boldsymbol{\omega} + \boldsymbol{\Lambda}\,\delta\boldsymbol{q}_{13} = \boldsymbol{0} \tag{14}$$

where $\boldsymbol{\Lambda}$ is a diagonal matrix with positive elements.

It will be shown that the spacecraft motion on a 3-dimensional sliding surface in the 6-dimensional state space of the vector part of the attitude error quaternion $\delta\boldsymbol{q}_{13}$ and the spacecraft angular velocity $\boldsymbol{\omega}$ is stable. From the definition of sliding surface, in Equation (14), we will show the convergence of $\delta\boldsymbol{q}_{13}$ to zero and δq_4 to 1 with an exponential decay.

Let us choose the following Lyapunov candidate function:

$$V_s = \delta\boldsymbol{q}_{13}^T\delta\boldsymbol{q}_{13} + (1-\delta q_4)^2 \tag{15}$$

From the quaternion normalization constraint, $\delta\boldsymbol{q}_{13}^T\delta\boldsymbol{q}_{13} + \delta q_4^2 = 1$, Equation (15) can be rewritten as

$$V_s = 2(1-\delta q_4) \tag{16}$$

Applying Equation (10b), the time derivative of the Lyapunov candidate function, Equation (16) is given by

$$\dot{V}_s = -2\delta\dot{q}_4 = \boldsymbol{\omega}^T\delta\boldsymbol{q}_{13} \tag{17}$$

Using the sliding vector in Equation (14), Equation (17) can be rewritten as

$$\dot{V}_s = -\delta\boldsymbol{q}_{13}^T\boldsymbol{\Lambda}^T\delta\boldsymbol{q}_{13} = -\delta\boldsymbol{q}_{13}^T\boldsymbol{\Lambda}\,\delta\boldsymbol{q}_{13} \tag{18}$$

The time derivative of the Lyapunov function is negative definite, since $\boldsymbol{\Lambda}$ is the positive definite matrix.

It should be noted that the equilibrium $\delta\boldsymbol{q} = [0 \quad 0 \quad 0 \quad -1]^T$, $\boldsymbol{\omega} = \boldsymbol{0}$ is stable. Furthermore, if the sliding surface is defined as,

$$\boldsymbol{s} = \boldsymbol{\omega} - \boldsymbol{\Lambda}\,\delta\boldsymbol{q}_{13} = \boldsymbol{0} \tag{19}$$

It is possible to show that the equilibrium $\delta\boldsymbol{q} = [0 \quad 0 \quad 0 \quad -1]^T$, $\boldsymbol{\omega} = \boldsymbol{0}$ is stable by using the following Lyapunov candidate function

$$V_s = \delta\boldsymbol{q}_{13}^T\delta\boldsymbol{q}_{13} + (1+\delta q_4)^2 \tag{20}$$

Now, we redefine the sliding surface as,

$$\boldsymbol{s} = \boldsymbol{\omega} + sign(\delta q_4)\boldsymbol{\Lambda}\,\Xi^T(\boldsymbol{q}_d)\boldsymbol{q} = \boldsymbol{\omega} + sign(\delta q_4)\boldsymbol{\Lambda}\,\delta\boldsymbol{q}_{13} = \boldsymbol{0} \tag{21}$$

As described the above, one can notice that the equilibrium becomes $\delta \boldsymbol{q} = [0\ \ 0\ \ 0\ \ -1]^T$ for $\delta q_4 < 0$, and the equilibrium becomes $\delta \boldsymbol{q} = [0\ \ 0\ \ 0\ \ 1]^T$ for $\delta q_4 > 0$. In other words, the sliding surface is selected depending on δq_4, and the state reaches the nearest equilibrium regarding δq_4.

2. Sliding condition design

The attraction of the sliding surface is assured by enforcing the sliding mode existence condition, which for a single input case are given by the following relations [3]:

$$\lim_{s \to 0^+} \frac{d}{dt} s < 0 \tag{22a}$$

$$\lim_{s \to 0^-} \frac{d}{dt} s > 0 \tag{22b}$$

For a general vector-valued case, Equation (22) is replaced with the Lyapunov condition below [3]:

$$\frac{d}{dt} \| \boldsymbol{s} \|^2 = 2\boldsymbol{s}^T \frac{d\boldsymbol{s}}{dt} < 0 \tag{23}$$

As described previously, the sliding mode controller is implemented to enforce the spacecraft motion towards the sliding surface, and track a desired quaternion $\boldsymbol{q}_d$.

Generally, the spacecraft attitude motion is not on the sliding surface, a desired control torque consists of the sum of an equivalent control and a part making the sliding vector converges to **0** in a finite time. If the attitude motion is on the sliding surface, the equivalent torque is the control torque necessary to maintain the attitude motion on the sliding surface. The sliding mode controller design with external torques is given by

$$\begin{aligned} \boldsymbol{u} &= -\boldsymbol{J}\left\{ f(\boldsymbol{\omega}) + \frac{1}{2} sign(\delta q_4) \boldsymbol{\Lambda} \left(\delta q_4 \boldsymbol{I}_{3\times 3} + [\delta \boldsymbol{q}_{13} \times] \right) \boldsymbol{\omega} \right\} - \boldsymbol{K}\boldsymbol{s} - \boldsymbol{P} sign(\boldsymbol{s}) \\ &= [\boldsymbol{\omega}\times]\boldsymbol{J}\boldsymbol{\omega} - \frac{1}{2} sign(\delta q_4) \boldsymbol{J}\boldsymbol{\Lambda} \left(\delta q_4 \boldsymbol{I}_{3\times 3} + [\delta \boldsymbol{q}_{13} \times] \right) \boldsymbol{\omega} - \boldsymbol{K}\boldsymbol{s} - \boldsymbol{P} sign(\boldsymbol{s}) \end{aligned} \tag{24}$$

where $\boldsymbol{K}$ and $\boldsymbol{P}$ are any positive definite diagonal matrices of designer-selected weights, and the equivalent control torque, $\boldsymbol{u}_{eq}$, is given by

$$\boldsymbol{u}_{eq} = -\boldsymbol{J}\left\{ f(\boldsymbol{\omega}) + \frac{1}{2} sign(\delta q_4) \boldsymbol{\Lambda} \left(\delta q_4 \boldsymbol{I}_{3\times 3} + [\delta \boldsymbol{q}_{13} \times] \right) \boldsymbol{\omega} \right\} \tag{25}$$

$\boldsymbol{K}$ and $\boldsymbol{P}$ assure the two conditions for sliding. $\boldsymbol{K}$ is effective for large $\boldsymbol{s}$ and $\boldsymbol{P}$ is dominant for small $\boldsymbol{s}$.

Using the sliding surface Equation (21), the time derivative of the sliding vector becomes

$$\frac{d\boldsymbol{s}}{dt} = \dot{\omega} + sign(\delta q_4) \boldsymbol{\Lambda}\, \delta\, \dot{\boldsymbol{q}}_{13} \tag{26}$$

Applying Equation (10a) and (11), Equation (26) is also given by

$$\frac{d\boldsymbol{s}}{dt} = f(\boldsymbol{\omega}) + \boldsymbol{J}^{-1}\boldsymbol{u} + sign(\delta q_4) \boldsymbol{\Lambda} \left(\frac{1}{2} \delta q_4 \boldsymbol{\omega} + \frac{1}{2} [\delta \boldsymbol{q}_{13} \times] \boldsymbol{\omega} \right) \tag{27}$$

Using the sliding mode controller given by Equation (24), Equation (27) then becomes

$$\begin{aligned} \frac{d\mathbf{s}}{dt} &= f(\omega) - f(\omega) - \frac{1}{2} sign(\delta \mathbf{q}_4) \Lambda \left(\delta q_4 \mathbf{I}_{3\times 3} + [\delta \mathbf{q}_{13} \times] \right) \omega \\ &\quad - \mathbf{J}^{-1} \left(\mathbf{K}\mathbf{s} + \mathbf{P} sign(\mathbf{s}) \right) + sign(\delta q_4) \Lambda \left(\frac{1}{2} \delta q_4 \omega + \frac{1}{2} [\delta \mathbf{q}_{13} \times] \omega \right) \\ &= -\mathbf{J}^{-1} \left(\mathbf{K}\mathbf{s} + \mathbf{P} sign(\mathbf{s}) \right) \end{aligned} \tag{28}$$

Using Equation (28), one can easily see that the sliding mode existence condition in Equation (23) is satisfied, given by

$$\frac{d}{dt} \| \boldsymbol{s} \|^2 = -\boldsymbol{s}^T \boldsymbol{J}^{-1} \left(\boldsymbol{K}\boldsymbol{s} + \boldsymbol{P} sign(\boldsymbol{s}) \right) < 0 \tag{29}$$

The saturation function $sat(\boldsymbol{s}, \varepsilon)$, used to reduce chattering in the control torques, is defined by

$$sat(\boldsymbol{s}, \varepsilon) \equiv \begin{cases} sign(s_i) & \text{if } | s_i | > \varepsilon \\ \dfrac{s_i}{\varepsilon} & \text{if } | s_i | \le \varepsilon \end{cases} \quad i = 1, 2, 3 \tag{30}$$

where $\varepsilon > 0$ is the "boundary layer thickness."

IV. Robustness

Now we consider disturbance and uncertainty to the robustness characteristic of sliding mode controller. We consider the system (11) with disturbance and uncertainty as the following

$$\dot{\boldsymbol{\omega}} = f + \Delta f + (G + \Delta G)\boldsymbol{u}(t) + d(t) \tag{31}$$

where G corresponds to $\boldsymbol{J}^{-1}$. In Equation (31), f and Δf are nonlinear driving term and their uncertainties, G and ΔG are the control gain and its uncertainty, and $d(t)$ and $\boldsymbol{u}(t)$ represent external disturbances and control signals. Furthermore Δf, ΔG and $d(t)$ are assumed to be bounded by known, continuous functions, i.e.

$$\left. \begin{aligned} | \Delta f | &\le F(t) \\ | \Delta G | &\le \Gamma(t) \\ | d | &\le D(t) \end{aligned} \right\} \tag{32}$$

Due to the disturbance and uncertainty, the time derivative of the sliding vector in Equation (26) needs to be modified to

$$\begin{aligned} \frac{d\boldsymbol{s}}{dt} = \dot{\boldsymbol{s}} &= -\boldsymbol{J}^{-1}(\boldsymbol{K}\boldsymbol{s} + \boldsymbol{P} sign(\boldsymbol{s})) + \Delta f + d + \Delta G\boldsymbol{u} \\ &= -\boldsymbol{J}^{-1}\boldsymbol{K}\boldsymbol{s} - \boldsymbol{J}^{-1}\boldsymbol{P} sign(\boldsymbol{s}) + \Delta f + d + \Delta G\boldsymbol{u} \end{aligned} \tag{31}$$

The following selection is sufficient to ensure the sliding mode existence condition in Equation (23).

$$\lambda_{J^{-1}P} = F + \Gamma \,|\, \boldsymbol{u} \,| + D \ge | \Delta f + d + \Delta G\boldsymbol{u} | \tag{34}$$

where $\lambda_{J^{-1}P}$ is the minimum singular value of the matrix $\boldsymbol{J}^{-1}\boldsymbol{P}$.

V. Actuator dynamics

There are several ways of producing torque for the attitude control of spacecraft. The use of momentum exchange devices, such as reaction wheels, momentum wheels, and control moment gyros(CMGs), provides angular momentum exchange between parts of the spacecraft without changing overall inertial angular momentum. For very accurate attitude control systems and for moderately fast maneuvers, the reaction wheels are preferred because they allow continuous and smooth control. The range of achievable torques with reaction wheels is of the order of 0.01 – 2 N-m.

The actuator system that we shall discuss here is a reaction wheel. Conventionally the reaction wheel is a DC motor and can be mounted in the spacecraft with its rotational axis in any direction relative to the spacecraft's axis frame.

The differential equation for the armature of the DC motor circuit is given by [7]

$$L_a \frac{di_a}{dt} + R_a i_a + K_b \Omega = e_a \tag{35}$$

where R_a is the armature resistance(*ohm*), L_a is the armature inductance(*henry*), K_b the is back emf constant, Ω is the angular velocity of motor(*rad/sec*), and i_a, e_a are the armature current(*ampere*) and applied armature voltage (*volt*) respectively.

In Equation (35), $K_b\Omega$ is the back emf which is the induced voltage in the armature proportional to the product of the flux and angular velocity. For a constant flux, the induced voltage e_b is directly proportional to the angular velocity, or

$$e_b = K_b \frac{d\theta}{dt} \tag{36}$$

where θ the is angular displacement of the motor shaft(*radian*).

The torque τ developed by the motor becomes directly proportional to the armature current so that

$$\tau = K_m i_a \tag{37}$$

where K_m is the motor torque constant(*N-m/A*).

The armature current produces the torque that is applied to the inertia and friction:

$$J_w \dot{\Omega} + b\Omega = \tau = K_m i_a \tag{38}$$

where J_w is the moment of inertia of the motor(*kg-m²*) and b is the viscous-friction coefficient of the motor(*N-m/rad/sec*).

Assuming that all initial conditions are zero and considering $E_a(s)$ as the input and $\Theta(s)$ as the output, and taking the Laplace transforms of Equations (35), (36) and (38), the transfer function for the DC motor is obtained as the following:

$$\frac{\Theta(s)}{\mathrm{E}_a(s)} = \frac{K_m}{s[L_a J_w s^2 + (L_a b + R_a J_w)s + R_a b + K_m K_b]} \tag{39}$$

The inductance L_a in the armature circuit is usally small and may be neglected. If L_a is neglected, then the transfer function given by Equation (39) reduces to

$$\frac{\Theta(s)}{\mathrm{E}_a(s)} = \frac{K_t}{s(T_m s + 1)} \tag{40}$$

where,

$K_t = K_m / (R_a b + K_m K_b)$: motor gain constant

$T_m = R_a J_w (R_a b + K_m K_b)$: motor time constant

Notice that from Equation (40), the differential equation for the motor system is given by

$$\ddot{\theta} + \frac{1}{T_m}\dot{\theta} = \frac{K_t}{T_m} e_a \tag{41}$$

Equation (41) can be rewritten as

$$\dot{\Omega} + \frac{1}{T_m}\Omega = \frac{K_t}{T_m} e_a \tag{42}$$

$$J_w \dot{\Omega} + \frac{J_w}{T_m}\Omega = J_w \frac{K_t}{T_m} e_a \tag{43}$$

If the spacecraft is equipped with 3 orthogonal reaction wheels, then the Euler's equations becomes by using Equation (43) for the wheel dynamics.

$$(\boldsymbol{J} - \boldsymbol{J}_w)\dot{\boldsymbol{\omega}} = -\boldsymbol{\omega} \times (\boldsymbol{J\omega} + \boldsymbol{J}_w \boldsymbol{\Omega}) - \bar{\boldsymbol{u}} \tag{44a}$$

$$\boldsymbol{J}_w(\dot{\boldsymbol{\omega}} + \dot{\boldsymbol{\Omega}}) = \boldsymbol{J}_w \frac{\boldsymbol{K}_t}{\boldsymbol{T}_m} \boldsymbol{e}_a - \frac{\boldsymbol{J}_w}{\boldsymbol{T}_m}(\boldsymbol{\Omega} + \boldsymbol{\omega}) = \bar{\boldsymbol{u}} \tag{44b}$$

where $\boldsymbol{J}_w$ is the diagonal inertia matrix of the wheels, $\boldsymbol{\Omega}$ is the wheel angular velocity vector, $\bar{\boldsymbol{u}}$ is the wheel torque vector, and $\boldsymbol{K}_t$, $\boldsymbol{T}_m$ are the diagonal matrix of the motor gain constant and motor time constant, respectively.

From the Equation (24), the sliding mode controller for the spacecraft equipped with wheels is given by the following:

$$\begin{aligned} \bar{\boldsymbol{u}} &= -[\boldsymbol{\omega}\times](\boldsymbol{J\omega} + \boldsymbol{J}_w\boldsymbol{\Omega}) + \frac{1}{2} sign(\delta q_4)(\boldsymbol{J} - \boldsymbol{J}_w)\boldsymbol{\Lambda}\left(\delta q_4 \boldsymbol{I}_{3\times3} + [\delta \boldsymbol{q}_{13}\times]\right)\boldsymbol{\omega} \\ &\quad + \boldsymbol{Ks} + \boldsymbol{P} sign(\boldsymbol{s}) \\ &= \boldsymbol{\Psi} \end{aligned} \tag{45}$$

The stability of the system can also be easily proven by using the Lyapunov condition in Equation (23).

The time derivative of the sliding vector Equation (26) is rewritten and given by

$$\frac{d\boldsymbol{s}}{dt} = \dot{\omega} + sign(\delta q_4)\boldsymbol{\Lambda}\delta\,\dot{\boldsymbol{q}}_{13} \tag{46}$$

Applying Equation (10a) and (44a), Equation (46) is also given by

$$\begin{aligned} \frac{d\boldsymbol{s}}{dt} &= (\boldsymbol{J} - \boldsymbol{J}_w)^{-1}\left(-\boldsymbol{\omega}\times(\boldsymbol{J\omega} + \boldsymbol{J}_w\boldsymbol{\Omega}) - \bar{\boldsymbol{u}}\right) \\ &\quad + sign(\delta q_4)\boldsymbol{\Lambda}\left(\frac{1}{2}\delta q_4 \boldsymbol{\omega} + \frac{1}{2}[\delta \boldsymbol{q}_{13}\times]\boldsymbol{\omega}\right) \end{aligned} \tag{47}$$

Equation (47) becomes by using the sliding mode controller as in Equation (45)

$$\begin{aligned} \frac{d\boldsymbol{s}}{dt} &= (\boldsymbol{J} - \boldsymbol{J}_w)^{-1}\{ -\boldsymbol{\omega}\times(\boldsymbol{J\omega} + \boldsymbol{J}_w\boldsymbol{\Omega}) + \boldsymbol{\omega}\times(\boldsymbol{J\omega} + \boldsymbol{J}_w\boldsymbol{\Omega}) \\ &\quad - \frac{1}{2} sign(\delta q_4)(\boldsymbol{J} - \boldsymbol{J}_w)\boldsymbol{\Lambda}\left(\delta q_4 + \frac{1}{2}[\delta \boldsymbol{q}_{13}\times]\right)\boldsymbol{\omega} - \boldsymbol{Ks} - \boldsymbol{P} sign(\boldsymbol{s}) \} \\ &\quad + sign(\delta q_4)\boldsymbol{\Lambda}\left(\frac{1}{2}\delta q_4 \boldsymbol{\omega} + \frac{1}{2}[\delta \boldsymbol{q}_{13}\times]\boldsymbol{\omega}\right) \\ &= -(\boldsymbol{J} - \boldsymbol{J}_w)^{-1}\left(\boldsymbol{Ks} + \boldsymbol{P} sign(\boldsymbol{s})\right) \end{aligned} \tag{48}$$

Using Equation (48), one can easily know that the sliding mode existence condition in Equation (23) is satisfied and given by

$$\frac{d}{dt}\| \boldsymbol{s} \|^2 = -\boldsymbol{s}^T(\boldsymbol{J}-\boldsymbol{J}_w)^{-1}\left(\boldsymbol{K}\boldsymbol{s}+\boldsymbol{P}sign(\boldsymbol{s})\right)<0 \qquad (49)$$

From Equations (44b) and (45), the voltage inputs to the wheel become

$$\boldsymbol{e}_a = \frac{\boldsymbol{T}_m}{\boldsymbol{K}_t\boldsymbol{J}_w}\left\{\boldsymbol{\Psi}+\frac{\boldsymbol{J}_w}{\boldsymbol{T}_m}(\boldsymbol{\Omega}+\boldsymbol{\omega})\right\} \qquad (50)$$

Considering Equations (44), (45) and (50), the stability of the system with wheels can be easily proven by using the Lyapunov condition in Equation (23).

VI. Simulation

An example of a three-axis spacecraft maneuver is presented, and the simultaneous reorientation of all axes is considered here, with the following inertia matrix taken from [3].

$$\boldsymbol{J} = diag[114 \quad 86 \quad 87]\ kg\text{-}m^2$$

The other initial conditions and design parameters are the following:

$$\boldsymbol{q}(t_0) = [0 \quad 0 \quad 0 \quad 1]^T$$
$$\boldsymbol{q}_d = [0.4423 \quad 0.4423 \quad 0.4423 \quad 0.6428]^T$$
$$\boldsymbol{\omega}(t_0) = [0.001 \quad 0.005 \quad 0.001]^T \ rad/sec$$
$$\boldsymbol{K} = 10\boldsymbol{I}_{3\times3},\ \boldsymbol{P} = 0.2\boldsymbol{I}_{3\times3},\ \boldsymbol{\Lambda} = 0.2\boldsymbol{I}_{3\times3}$$
$$\boldsymbol{J}_w = diag[0.0077 \quad 0.0077 \quad 0.0077]\ kg\text{-}m^2$$
$$R_a = 1\ (ohm),\ K_b = 0.0001,\ K_m = 0.1\ (N\text{-}m/A)$$

viscous friction : 1.21e-6 (*N-m/rad/sec*)

$$\boldsymbol{\Omega}(t_0) = [0 \quad 0 \quad 0]^T \ rad/sec$$

And the boundary layer thickness is set to $\varepsilon = 0.001$ and the input voltage to wheels is limited to 5(V). Also, the control torque of the wheels is limited to 1.0 N-m.

To show the robustness of the controller, disturbance torques are assumed to be

$$d(t) = [0.005\sin(0.05t) \quad 0.003\cos(0.05t) \quad -0.005\sin(0.05t)]^T \text{ N-m}$$

The matrix $\boldsymbol{P} = 0.3\boldsymbol{I}_{3\times3}$ is chosen to satisfy the condition defined by Equation (34).

Fig. 1 depicts the time trajectories of the error quaternions and shows the convergence of $\delta\boldsymbol{q}_{13}$ to zero and δq_4 to 1. Fig. 2 shows the angular velocity of spacecraft. Fig. 3 shows the switching function trajectories in presence of disturbance. The plot of the input voltge to the wheels and the control torque are shown in Fig. 4 and 5, respectively. From Fig. 1 to Fig. 3, one can know that the controller accommodate the external disturbance torques. As described in section IV, if $\lambda_{J^{-1}P}$ is chosen to satisfy the robustness condition given by Equation (34), the controller is also robust to parameter variation and unmodelled effects.

We select $\boldsymbol{q}_d = [-0.4423 \quad -0.4423 \quad -0.4423 \quad -0.6428]^T$ to show the equilibrium $\delta\boldsymbol{q} = [0 \quad 0 \quad 0 \quad -1]^T$ is stable for $\delta q_4 < 0$. From the Fig. 6, one can notice that the controller drives the system toward the equilibrium $\delta\boldsymbol{q} = [0 \quad 0 \quad 0 \quad -1]^T$ for $\delta q_4 < 0$. Fig. 7 and Fig. 8 show the time trajectories of the error quaternion and the swiching function when $sign(\delta q_4)$ is not considered. In this case, the controller enforces the system toward the equilibrium $\delta\boldsymbol{q} = [0 \quad 0 \quad 0 \quad 1]^T$ for $\delta q_4 < 0$. So it requires more control effors to reach the sliding surface and the equilibrium. As a result, one can know that using $sign(\delta q_4)$ assures the state reaches the nearest equillibrium of $\delta\boldsymbol{q}$.

VII. Conclusions

The problem of sliding mode control of spacecraft with actuator dynamics is studied for real applications. The controller is derived based on quaternion, and the analysis of robustness is presented for the derived control scheme in the presence of unmodeled effects and disturbances. For a real-application, actuator dynamics, especially reaction wheels, is studied. The reaction wheel dynamic equation represented by the wheel

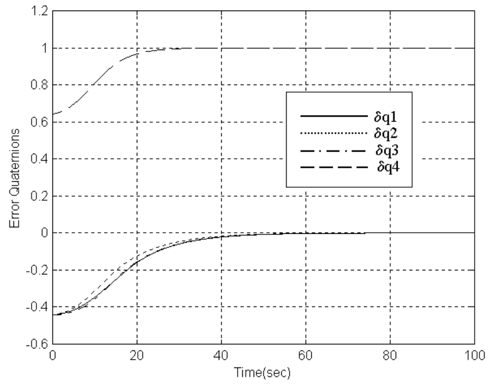

Fig. 1. Plot of Error Quaternion Trajectories.

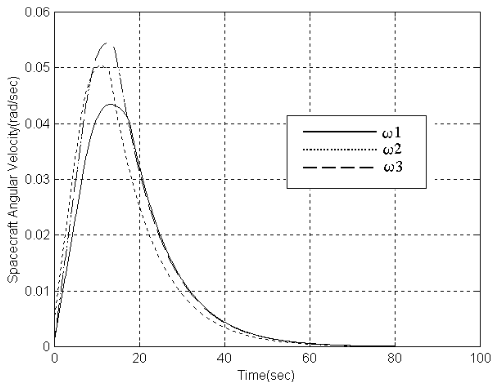

Fig. 2. Plot of Angular Velocity Trajectories.

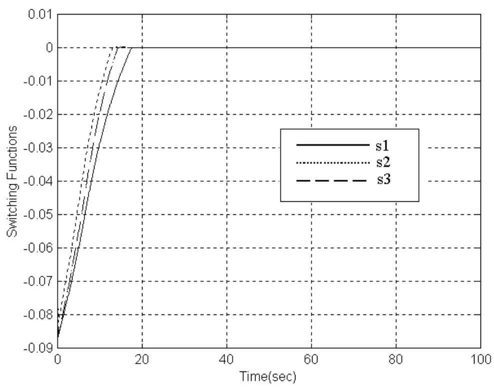

Fig. 3. Plot of switching function trajectories.

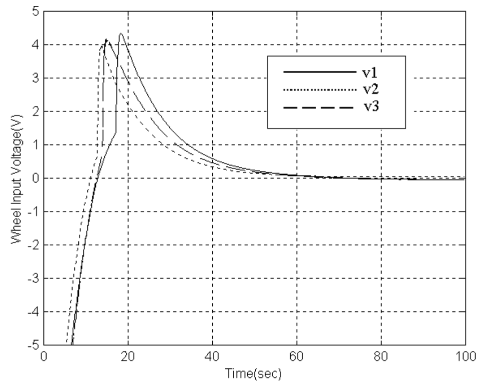

Fig. 4. Plot of Wheel Input Voltage Trajectories.

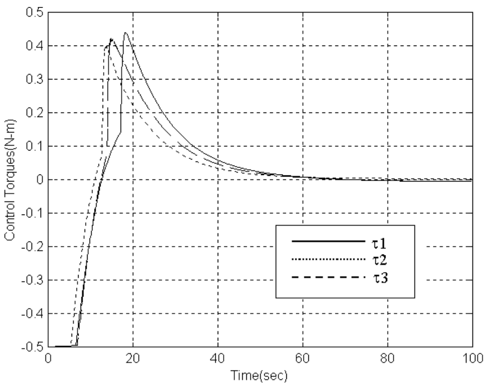

Fig. 5. Plot of Control Torque Trajectories.

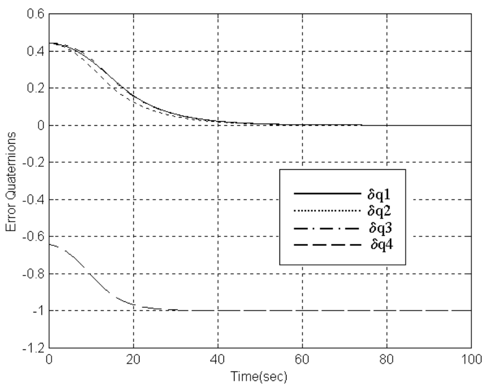

Fig. 6. Plot of Error Quaternion Trajectories for $\boldsymbol{q}_d = [-0.4423 \quad -0.4423 \quad -0.4423 \quad -0.6428]^T$.

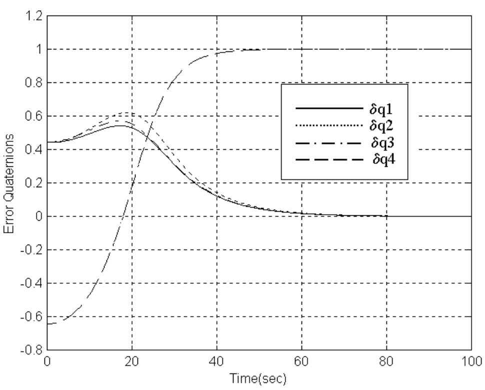

Fig. 7. Plot of Error Quaternion Trajectories for $\boldsymbol{q}_d = [-0.4423 \quad -0.4423 \quad -0.4423 \quad -0.6428]^T$ without considering $sign(\delta q_4)$.

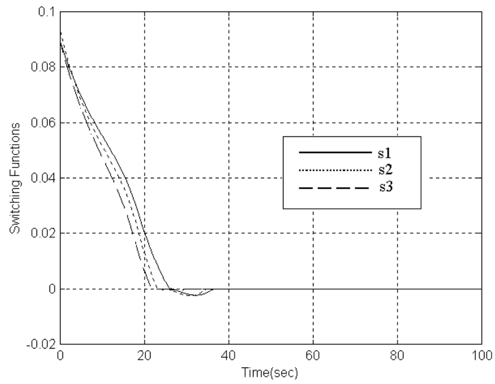

Fig. 8. Plot of Switching Function Trajectories for $\boldsymbol{q}_d = [-0.4423 \quad -0.4423 \quad -0.4423 \quad -0.6428]^T$ without considering $sign(\delta q_4)$.

input voltage. And we present the wheel input voltage based on the sliding mode controller and derived reaction wheel dynamic equation. Simulation results show that the control system performs acceptably in the presence of external disturbances.

References

[1] J. L. Crassidis, S. R. Vadali, F. L. Markey, "Optimal variable-structure control tracking of spacecraft maneuvers," *Journal of Guidance, Control, and Dynamics*, vol. 23, no. 3, pp. 564-566, May-June, 2000.

[2] V. I. Utkin, *Sliding Mode in Control Optimization*, Springer-Verlag, Heidelberg, 1992.

[3] T. A. W. Dwyer, H. Ramirez, "Variable-structure control of spacecraft attitude maneuvers," *Journal of Guidance, Control, and Dynamics*, vol. 11, no. 3, pp. 262-270, May-June 1988.

[4] J. L. Crassidis, F. L. Markley, "Sliding mode control using modified rodrigues parameters," *Journal of Guidance, Control, and Dynamics*, vol. 19, no. 6, pp. 1381-1383, Nov.-Dec., 1996.

[5] S. R. Vadali, "Variable-structure control of spacecraft large-angle maneuvers," *Journal of Guidance, Control, and Dynamics*, vol. 9, pp. 235-239, 1986.

[6] H. Ramirez, *Nonlinear Pulse Width Modulation Controller Design,* Variable Structure Control for Robotics and Aerospace Applications, pp. 33-58, Elsevier, 1993.

[7] K. Ogata, *Modern Control Engineering*, 2nd Edition, Prentice-Hall, 1990.

[8] Y. J. Cheon, "Sliding mode control for attitude tracking of thruster-controlled spacecraft," *ICASE Transactions on Control, Automation and Systems Engineering*, vol. 3, no. 4, pp. 257-261, December, 2001.

Yee-Jin Cheon

He was born in Korea on January 15, 1970. He received B.S and M.S degrees from School of Electrical Engineering and Computer Science, Kyungpook National University, Korea in 1993 and 1995. He participated in Korea Government satellite project-KOMPSAT-1(Korea Multi-Purpose SATellite-1) from 1995 to 1999. Currently he is involved in KOMPSAT-2 project as a flight software engineer. He is a senior researcher of Korea Aerospace Research Institute, Korea. His research interests are real-time software for control, variable structure control of spacecraft attitude tracking and unscented Kalman filter for nonlinear estimation.